FULL TITLE
ASP Conference Series, Vol. **VOLUME**, **YEAR OF PUBLICATION**
NAMES OF EDITORS

Rotation and Mass Loss

Stan Owocki
Bartol Research Institute, Department of Physics & Astronomy, University of Delaware, Newark, DE 19716

Abstract. Stellar rotation can play an important role in structuring and enhancing the mass loss from massive stars. Initial 1D models focussed on the expected centrifugal enhancment of the line-driven mass flux from the equator of a rotating star, but the review here emphasizes that the loss of centrifugal support away from the stellar surface actually limits the steady mass flux to just the point-star CAK value, with models near critical rotation characterized by a slow, subcritical acceleration. Recent suggestions that such slow outflows might have high enough density to explain disks in Be or B[e] stars are examined in the context of 2D simulations of the "Wind Compressed Disk" (WCD) paradigm, together with a review of the tendency for poleward components of the line-driving force to inhibit WCD formation. When one accounts for equatorial gravity darkening, the net tendency is in fact for the relatively bright regions at higher latitude to drive a faster, denser "bipolar" ouflow. I discuss the potential relevance for the bipolar form of nebulae from LBV stars like eta Carinae, but emphasize that, since the large mass loss associated with the eruption of eta Carinae's Homunculus would heavily saturate line-driving, explaining its bipolar form requires development of analogous models for continuum-driven mass loss. I conclude with a discussion of how radiation seems inherently ill-suited to supporting or driving a geometrically thin, but optically thick disk or disk outflow. The disks inferred in Be and B[e] stars may instead be centrifugally ejected, with radiation inducing an ablation flow from the disk surface, and thus perhaps playing a greater role in destroying (rather than creating) an orbiting, circumstellar disk.

1. Introduction

At some level, all stars both rotate and lose mass. Typical of most cool stars, our Sun has a quite slow equatorial rotation speed of ca. 1 km/s, and also a quite low mass loss rate of ca. $10^{-14} M_\odot$/yr. By contrast, for the hot, luminous, massive stars that are a principal focus of this meeting (and of Henny Lamers' research), both rotation rates and mass loss rates are generally much larger and span a much wider range. The rotational broadening of photospheric lines in such hot stars generally imply projected equatorial rotation speeds (Vsin(i)) measured in tens or hundreds of km/s, sometimes (e.g. in Be stars) even approaching the "critical" rotation speed (ca. 400-500 km/s) at which the equatorial surface would effectively be in Keplerian orbit. And hot-star mass loss rates range from ca. $10^{-10} M_\odot$/yr (for mid-to-late B-stars) to ca. $10^{-5} M_\odot$/yr for Wolf-Rayet (WR) stars, to even ca. $1 M_\odot$/yr in extreme eruptions of Luminous Blue Variable (LBV) stars, e.g., the 1840-50 eruption of eta Carinae. Moreover, such mass loss often shows signs of being aspherical, sometimes with a prolate, bipolar

form (as in eta Carina), sometimes with a equatorial flattened disk (as in Be and B[e] stars), and sometimes with an episodic or periodic variability (as in the "Discrete Absorption Components" – DACs – seen in UV P-Cygni lines).

As discussed below, it seems that rotation likely plays a key role in such aspherical forms of mass loss, but the specifics of how this occurs can be quite subtle and even surprising. A key issue is how rotation alters the standard CAK (Castor et al. 1975) formalism for stellar wind mass loss driven by the line-scattering of the star's continuum radiation. Historically, some initial insights were gleaned from just adding centrigual terms to 1D models of the equatorial outflow (§2), but subsequent work has demonstrated the essential role of 2D and perhaps even 3D effects (§3). The review here aims to summarize these issues within a basic physical context.

2. 1D Models of Rotational Effects on an Equatorial CAK Wind

Initial analyses (Friend & Abbott 1986; Pauldrach et al. 1986, hereafter FA and PPK) of rotational effects on hot-star mass loss derived 1D models of the steady equatorial outflow based on the standard CAK line-driving formalism, but now adding the effect of an outward centrifugal acceleration. For purely radial driving without any torque, conservation of angular momentum requires that the product of radius r and azimuthal speed v_ϕ must remain fixed at the surface value imparted by the equatorial stellar rotation, $rv_\phi = R_{eq}V_{rot}$. The centrifugal acceleration thus varies as

$$g_{cent} = \frac{v_\phi^2}{r} = \frac{V_{rot}^2 R_{eq}^2}{r^3} \, . \tag{1}$$

This has the effect of reducing the net inward acceleration from gravity by a factor

$$1 - \frac{g_{cent}}{GM/R_{eq}^2} = 1 - \omega^2 \frac{R_{eq}}{r} \, , \tag{2}$$

where

$$\omega^2 \equiv \frac{V_{rot}^2 R_{eq}}{GM} \, , \tag{3}$$

with G the gravitation constant and M the stellar mass.

In the initial models that assumed a fixed surface brightness (i.e., ignoring the equatorial gravity darkening discussed in §3.3), this effective reduction of gravity makes it possible for the line-scattering to drive a greater mass flux from the rotating equatorial surface. However, because this centrifugal acceleration falls off faster than the $1/r^2$ decline of gravity, the loss of centrifugal support makes it harder for the outward acceleration of enhanced mass flux to be maintained at larger radii. At low and moderate rotation speed, the net effect is just to lower somewhat the wind terminal speed; but when FA attempted to extend their 1D models to very high rotation, they found that the standard CAK supercritical solutions with steep acceleration simply *terminated* beyond some finite radius. Over the past few years, there have been several additional 1D studies of the role of rotation on hot-star mass loss (Aerts & Lamers 2003; Aerts et al. 2004; Curé 2004; Curé & Rial 2004; Curé et al. 2005). The papers by M. Curé

and collaborators suggest that this mass overloading can induce a sudden switch to a much slower, "subcritical" wind solution, for which the high mass flux and low flow speed imply a much denser outflow, perhaps providing an explanation for the dense equatorial outflows seen in B[e] supergiants.

To clarify the underlying physical issues, let us summarize here key results of a simplified "nozzle" analysis of the steady, 1D equation of motion (Owocki 2006), supplemented by some 1D numerical hydrodynamics simulations (Madura et al. 1996). A key issue lies in the interaction of rotational effects with the so-called "finite-disk-correction-factor" (fdcf) for the line-driving. The initial CAK wind model was based on the idealization of radially streaming radiation, as if the star were a point source at the origin. CAK did already identify (but did not implement) the appropriate fdcf to account for the full angular extent of the star (see CAK eq. [50]). Its complex dependence on radius, velocity, and velocity gradient complicates the solution of the full equation of motion, but such finite-disk-corrected solutions were obtained independently by FA and PPK, in the same papers that also examined rotation effects in 1D models.

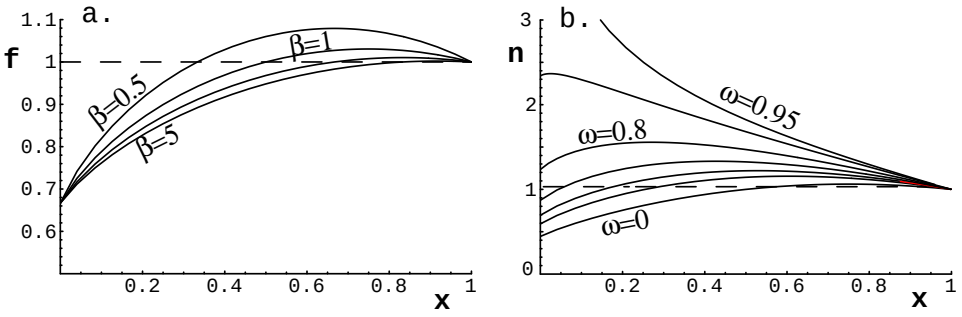

Figure 1. a. Spatial variation of the finite-disk-correction factor f, plotted vs. scaled inverse radius $x = 1 - R_{eq}/r$, for CAK exponent $\alpha = 1/2$ and various velocity-law exponents, $\beta = 0.5$, 1, 2, and 5. b. Nozzle function $n(x)$ plotted vs. inverse radius x, various rotation rates $\omega = 0$, 0.5, 0.6, 0.7, 0.8, 0.9, and 0.95, and using a $\beta = 1$ velocity law in evaluating the fdcf.

Figure 1a illustrates the typical spatial variation of this fdcf, plotted here as a function of the scaled inverse radius coordinate, $x \equiv 1 - R_{eq}/r$. To convert the complex implicit dependence on velocity and velocity gradient to an explicit spatial function, the computation assumes a canonical value for the CAK exponent $\alpha = 1/2$, and a simplified "beta-law" form for the velocity, $v(r) = v_\infty(1 - R_{eq}/r)^\beta$, with the various curves labeled by the assumed velocity index β. Note that these fdcf curves all have a quite similar overall form, starting from a reduced value $f_* = 1/(1+\alpha)$ near the stellar surface ($r = R_{eq}, x = 0$), then increasing past unity at the isotropic expansion radius (where $dv/dr = v/r$), $r/R_{eq} = (1+\beta)$, $x = \beta/(1+\beta)$, and eventually returning asymptotically to unity from above at large radii ($r \to \infty; x \to 1$), where the star does indeed become a point source.

Without rotation, the finite-disk reduction in line-driving near the stellar surface makes this region the most difficult for maintaining the flow acceleration, somewhat like the "throat" of a rocket nozzle. Compared to the point-star CAK model, the mass flux that can be driven through this near-surface throat is

reduced by a factor

$$\dot{m} \equiv \frac{\dot{M}}{\dot{M}_{CAK}} = f_*^{1/\alpha} = (1+\alpha)^{-1/\alpha} \,, \tag{4}$$

or a factor 4/9 for our canonical case $\alpha = 1/2$. The subsequent rise in the fdcf away from the surface then results in a kind of "after-burner" effect that increasses the wind acceleration, leading to a enhanced terminal wind speed, v_∞.

With rotation included, the effective centrifugal reduction in the near-surface gravity compensates for the lower line-driving from the fdcf factor, thus allowing again a larger surface mass flux. The combined net effect can be quantified in terms of a "nozzle function" (Owocki 2006; Madura et al. 1996), given for the $\alpha = 1/2$ case by

$$n(x) = \frac{f(x)^2}{1-\omega^2(1-x)} \,. \tag{5}$$

The significance of this nozzle function stems from its appearance with the mass flux $\dot{m}$ within a square-root discriminant in solutions for the wind acceleration. In particular, maintaining a numerically real flow acceleration requires a mass flux $\dot{m} \leq \min[n(x)]$. The location of the global minimum of this nozzle function (the smallest nozzle "throat") thus represents the *critical point* that sets the maximal allowed value of the mass flux, $\dot{m} = \min[n(x)]$, that is consistent with a monotonically accelerating outflow.

Figure 1b plots $n(x)$ vs. x for various rotation rates ω, using a $\beta = 1$ velocity law to obtain a spatially explicit approximation to the fdcf. Note that for no or low rotation (about $\omega < 0.75$), the minimum of the nozzle function is less than unity, and occurs at the stellar surface, $x = 0$. This allows the flow to transition to a *super*-critical outflow directly from the static surface boundary condition $v(R_{eq}) = 0$, following a steep solution root for the acceleration. The mass flux is greater than the finite-disk corrected value given in eqn. (4), but still less than the point-star CAK value,

$$\dot{m} = \dot{m}_0 \equiv n(x=0) \equiv \frac{f^2(x=0)}{1-\omega^2} = \frac{4/9}{1-\omega^2} \,, \tag{6}$$

where the factor 4/9 in the final numerator is just the $\alpha = 1/2$ value for the zero-rotation, finite-disk-corrected mass loss scaling derived by FA and PPK, as given here in eqn. (4).

Note, however, from eqn. (4) that for rotation rates above $\omega = \sqrt{5/9} \approx 0.75$, this local nozzle minimum at the base *exceeds* the unit value it approaches at large radii, $x = 1$. For such rapid rotation rates, maintaining an accelerating outflow thus requires limiting the mass flux to the point-star CAK value, $\dot{m} = 1$, with the flow kept to a relatively shallow *sub*-critical acceleration all the way to this global nozzle minimum at large radii, which now represents a kind of "outer critical point". This thus provides the basic explanation for the switch from steep to shallow accelerations inferred by Curé et al. (2005).

The associated wind velocity laws can be obtained by simple numerical integration of the steady 1D equation of motion from a static lower boundary.

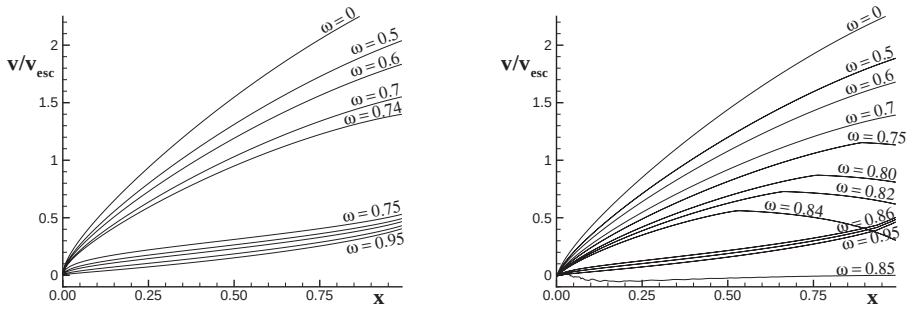

Figure 2. a. Flow speed over surface escape speed, $v/v_{\rm esc}$, plotted vs. scaled inverse radius $x = 1 - R_*/r$, as derived from a nozzle analysis, using a steep acceleration for no or modest rotation, $\omega \leq 0.74$, and shallow acceleration for rapid, near-critical rotation, $\omega \geq 0.75$. b. Same as in (a), but now obtained from asymptotic states of full hydrodynamical simulations. Note the overall good agreement, but with the transition from steep to shallow solutions bridged by a new kind of solution with a velocity gradient "kink".

Figure 2a plots the resulting velocity laws for selected slow vs. rapid rotation rates, yielding respectively the steep vs. shallow types of flow solution. Figure 2b compares analogous results for the asymptotic steady states of numerical hydrodynamics simulations based on the full 1D, time-dependent equation of motion. The remarkably close overall agreement confirms the basic validity of the simple nozzle analysis. But note that in the full hydrodynamical simulations the transition from steep to shallow solutions is bridged by a new kind of solution in which the steep CAK-type acceleration of an overloaded base mass flux ($\dot{m} > 0$) switches via an abrupt "kink" (discontinuity in velocity gradient) to a *declerating* solution. Analysis shows, in fact, that such kink transitions occur at essentially the very locations where FA found their CAK acceleration solutions to terminate. In the context of the nozzle analysis, this occurs where the local value of the nozzle function declines below the surface value that lead to an overloaded surface mass flux, i.e. at an inverse radius x_k given by $n(x_k) = n(x = 0) = \dot{m}_o > 1$.

For rotation rates $\omega \gtrsim 0.85$, this kink location becomes so close to the star that the post-kink deceleration causes the outflow to *stagnate* at a finite radius, with gravity then pulling this overloaded material back as a reaccretion onto the star. But quite remarkably, the subequent recovery is then characterized by a near-CAK mass flux that can now be sustained as a steady wind solution with slow, shallow acceleration. For sufficiently high rotation rates, $\omega \gtrsim 0.88$, the nozzle function declines monotonically from the surface, and in these cases the time-dependent simulations show the direct development of a slow solution without any intermediate kink phase.

Figure 3a summarizes the overall effect of rotation on the two key wind properties, namely the mass flux $\dot{m}$, and terminal wind v_∞, with each plotted as a function of the scaled rotation rate ω. As the rotation increases past the threshold rate at $\omega \approx 0.75$, the velocity shows an abrupt shift associated with

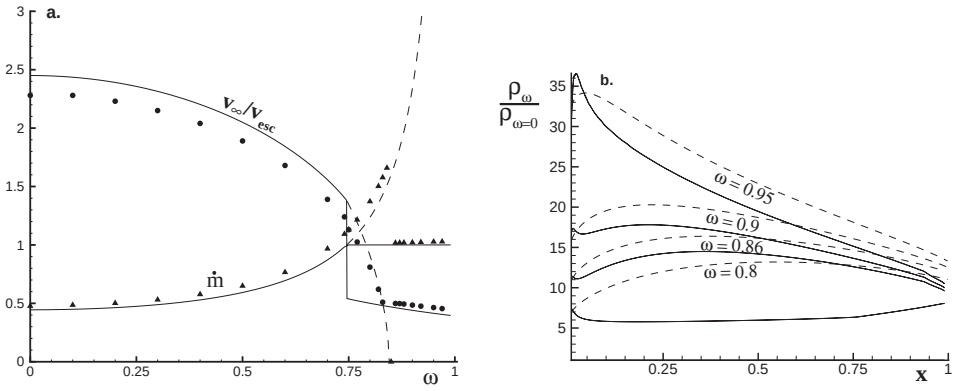

Figure 3. a. Terminal flow speed over surface escape speed (upper curve) and mass flux in units of point-star CAK value (lower curve), plotted vs. rotation rate ω, as derived by simple nozzle analysis. The circles and triangles compare corresponding hydro simulation results for respectively the terminal speed and mass flux. b. Density enhancement of slow wind solutions with various rapid rotation rates ω, relative to a non-rotating wind with the same parameters, and showing results from both a nozzle analysis (dashed curves) and numerical simulations (solid curves).

the switch from steep to shallow acceleration, with the mass flux saturating to the point-star CAK value, $\dot{m} = 1$. The dashed curves show extrapolated results if the local nozzle minimum at the surface is instead used to set flow conditions; the mass loss in this case is set by the scaling $\dot{m}_0$ in eq. (6), and the terminal speed is derived by assuming a pure gravitational coasting for all radii with $n(x) < \dot{m}_0$. The data points again compare corresponding results for the full dynamical simulation, as described above.

As emphasized by Curé et al. (2005), the shift to a much slower flow solution suggests, via mass continuity, that the equatorial regions of a rotating star should have a significantly enhanced density compared to its relatively fast, polar wind. These results then allow us to identify the radial variation of the relative density enhancement in the slow equatorial wind of a rotating star, compared to the non-rotating solution that applies to the polar wind. Assuming all other wind parameters to be fixed, figure 3b plots the spatial variation of the density relative to a non-rotating model, for various rapid rotation cases, as computed both with the simple nozzle analysis (dashed curves) and the full numerical hydro simulations (solid curves). Note that the enhancements are up to a few factors of ten, not insignificant, but perhap not really sufficient to reproduce the inferred equatorial densities of, e.g., supergiant B[e] disks. Moreover, it seems that ascertaining the broad physical relevance of such potentially slow, dense equatorial outflows requires taking account of the 2D latitudinal flow from higher latitudes, as we discuss next.

But it is perhaps worth emphasizing a key lesson of this 1D analysis, namely that the arbitrarily large base mass flux implied by a simple CAK scaling law for rotations approaching critical [e.g., eqn. (6) for $\omega \to 1$] are *not* physically realistic, since the loss of centrifugal support means such overloaded solutions

cannot be driven to full escape from the star. The maximum mass flux in such 1D rotation models is, in fact, just the point-star CAK value, which is only about a factor two above the finite-disk-corrected value for a non-rotating star (cf., Aerts & Lamers 2003).

3. 2D Dynamical Models of Rotating Line-Driven Winds

3.1. Equatorial Wind Compressed Disks

Extending such idealized 1D rotating wind models to account for multidimensional effects presents some formidable challenges.

Initial efforts (e.g., Poe 1987) centered on generalizing the 1D CAK critical solution analysis to a 2D axisymmetric model of the rotating wind, but obtaining direct, analogous solution of the coupled set of *partial* differential equations for the density and (now vector) velocity proved quite difficult.

A key conceptual breakthrough came through an insightful semi-analytic treatment by Bjorkman & Cassinelli (1993, hereafter BC), which led to the prediction that rapid rotation could channel wind outflow into a dense, equatorial *Wind Compressed Disk* (WCD). BC noted that, like satellites launched into earth orbit, parcels of gas gradually driven radially outward from a rapidly rotating star should remain in a tilted 'orbital plane' that brings them over the equator. As wind parcels from opposite hemispheres collide over the equator, they form a disk of compressed gas. A key simplification here is to assume that, like gravity, the radiative driving is a radially directed, *central* force. As such, the total angular momentum of each individual wind fluid parcel is conserved, fixed by the rotation at its initial latitude at the wind base (i.e., at the subsonic stellar surface), and remaining in a fixed plane perpendicular to the angular momentum vector. The crucial criterion for the formation of a disk is that the near-star wind speed not be too much larger than the rotation speed. For lower rotation or faster winds, material may not be deflected into a disk, but still can form a more modest equatorial density enhancement, a "Wind Compressed Zone" (WCZ; Ignace et al. 1996). BC proposed that the WCD mechanism could provide a natural explanation for the circumstellar disks inferred from rapidly rotating Be stars.

To test this WCD paradigm, Owocki et al. (1994) carried out 2D hydrodynamical simulations of line-driven winds from rotating hot-stars. In keeping with the original WCD model, they assumed a purely radial driving force, though now computed dynamically using the finite-disk, spherical-star form of the usual CAK line-driving force. The results confirmed the basic formation of equatorial disk flow, with density increasing with more rapid surface rotation speed, as shown in figure 4. The overall wind morphology consists of a relatively fast, low-density polar wind, plus a dense equatorial disk with slow outflow in its outer part, as well as an infall in the inner part. For the typical case of a B2 star with a surface rotation speed of 350 km/s, figure 5a shows density contours plotted vs. radius and colatitude, with superposed arrows representing the magnitude and sense of the latitudinal velocity component $v_\theta(r,\theta)$. The WCD, manifest here by the strong equatorial extension of higher density contours, is the direct result of the flow compression associated with the equatorward sense of the latitudinal velocity from both the northern and southern hemispheres.

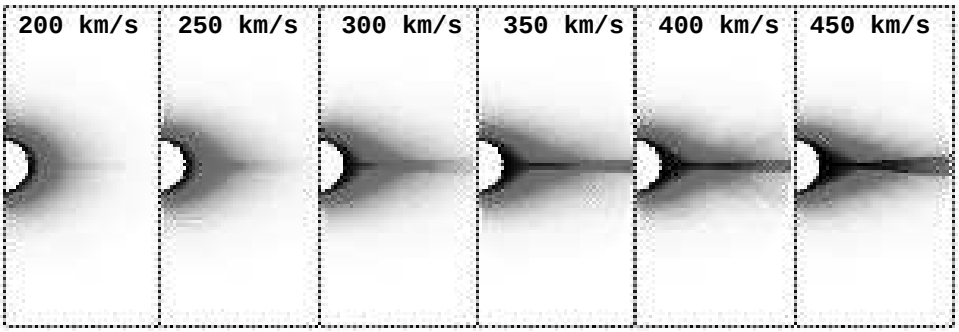

Figure 4. For the various labeled equatorial rotation speeds, greyscale plots of final-state density in 2D wind simulations that assume a purely radial form for the line-driving. The model has a critical rotation speed of 488 km/s.

However, because the outflow from a subcritically rotating star necessarily lacks the angular momentum for a stationary orbit, material in the inner disk is pulled by gravity into reaccretion back onto the star, while material in the outer disk flows outward with the stellar wind. This overall "leaking" of the WCD limits its density to values well below (by ca. a factor 100) that needed to explain either the observed Balmer emission or continuum polarization of Be-star disks (Bjorkman 1999). These substantial radial flow speeds also do not seem compatible with observed line-profile features, most notably the "central quasi-emissions" (Rivinius et al. 1999; Hanushik 1995). Finally, since this radially flowing WCD material has a characteristic residence time of only a few days, the WCD model seems inherently incapable of explaining the long-term (several year) variations of Violet/Red (V/R) emission peak asymmetries seen in many Be stars; instead these seem consistent with slow one-arm disk-oscillation modes that are grounded in the gradual precession of elliptical orbits within a Keplerian disk (Savonije & Heemskerk 1993; Telting et al. 1994; Savonije 1998).

Although it thus now seems quite clear that the WCD mechanism can not explain Be star emission, its introduction and development was nonetheless a quite important and instructive step forward, as one of the first dynamically based models of disk formation with falsifiable predictions. In particular, it highlighted that among key requirements for producing a viable disk are not just to propel material from the surface and focus it toward the equator, but rather also to provide it with sufficient angular momentum to maintain a Keplerian orbit.

3.2. Inhibition of WCD by Poleward Component of the Line-Force

For rotating stars, the line acceleration can generally also have *nonradial* components, arising from both the stellar oblateness and asymmetries in the velocity gradient, as illustrated respectively by the left and right panels of figure 6. Within the CAK formalism of a fixed ensemble of lines with a power-law number distribution in opacity, its vector form is given by integration over solid angle

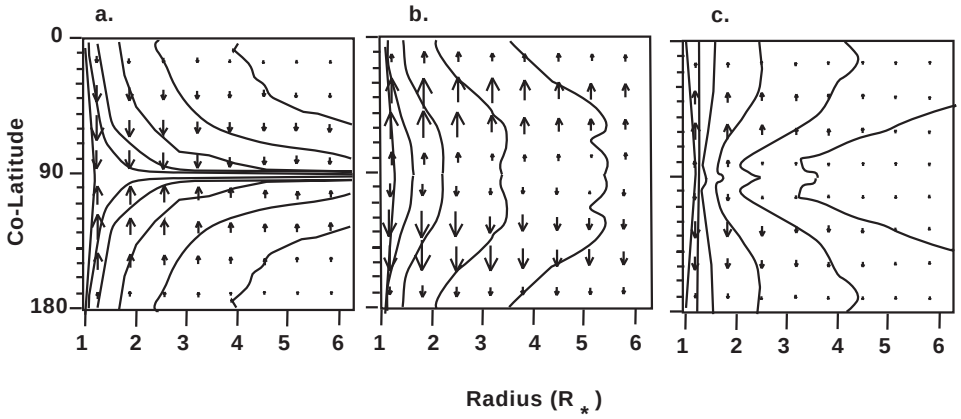

Figure 5. Contours of stellar wind density plotted vs. colatitude θ and radius r, for a standard B2 star model with equatorial rotation speed of 350 km/s. The superposed vectors represent the latitudinal velocity, with the maximum length corresponding to a magnitude of v_θ =100 km/s. The three panels show the cases (a) without nonradial forces or gravity darkening, (b) with nonradial forces but no gravity darkening, and (c) with both nonradial forces and gravity darkening.

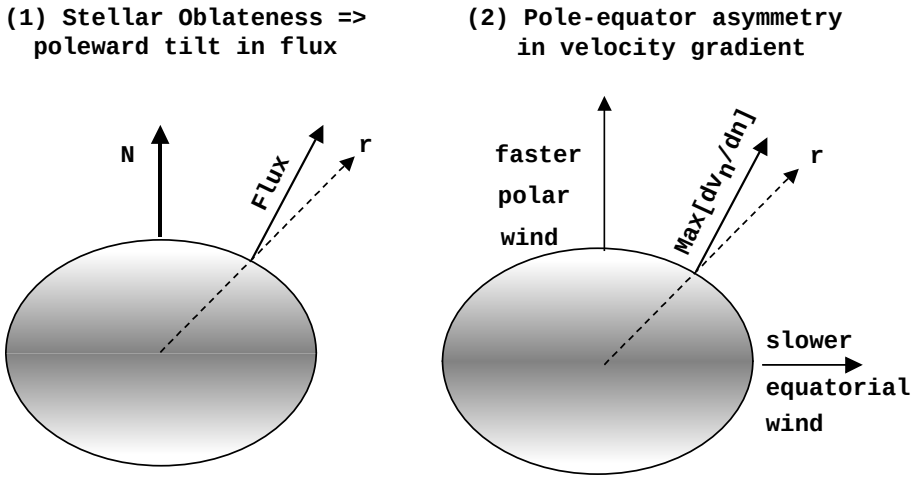

Figure 6. Illustration of the origin of poleward component of the radiative force from a rotating star. Left: The poleward tilt of the radiative flux arising from the oblateness of the stellar surface contributes to a poleward component of the driving force. Right: The lower effective gravity of the equator yields a slower equatorial speed, and the associated poleward tilt in the velocity gradient contributes further to a poleward component of the line force.

Ω_* of the stellar core intensity I (Cranmer & Owocki 1995),

$$\mathbf{g}^{\rm rad}(\mathbf{r}) \propto \int_{\Omega_*} d\Omega\, \mathbf{n}\, I(\mathbf{n},\mathbf{r})\, \{\mathbf{n}\cdot\nabla\,[\mathbf{n}\cdot\mathbf{v}(\mathbf{r})]\}^{\alpha}\ , \qquad (7)$$

where α is again the CAK exponent. Note that the weighting for the force contribution of each ray along a direction $\mathbf{n}$ is proportional to the projected velocity gradient in that direction, $\mathbf{n} \cdot \nabla [\mathbf{n} \cdot \mathbf{v}(\mathbf{r})]$.

Owocki et al. (1996) carried out 2D simulations of rotating winds including these nonradial line-force components. Figure 5b shows the corresponding wind density structure for the standard 350 km/s rotations model, still assuming a uniformly bright stellar core. As predicted in the above 1D analysis, the reduced gravity, enhanced mass loss, and lower flow speed near the equator yield a broad, moderate density enhancement in the equatorial wind. But there is *no wind compressed disk*. Indeed, the sense of the superposed vectors is now reversed, indicating that the latitudinal velocity is now *away from the equator*. As such, there is no longer any wind compression effect, and so the tendency to form a WCD is completely inhibited.

This latitudinal flow reversal is a direct consequence of a *poleward* component of the line-force. In part this arises from asymmetries in the line-of-sight velocity gradient, operating through the velocity-gradient weighting of the angle integral for the line force in eqn. (7). The lower effective gravity near the equator implies generally lower outflow speeds there, and thus from most mid-latitude locations in the wind, the line-of-sight velocity gradient is stronger when looking toward the equator than toward the pole. Hence, as illusrated in the right panel of figure 6, photons from near the equator impart a stronger impulse than those from near the pole, thus enhancing the net poleward component of the line-force. Moreover, as shown in the left panel of figure 6, near the oblate stellar surface, there arises an additional poleward force from the poleward tilt of the radiative flux. Even with both effects, the magnitude of this poleward force is quite small, generally not much more than 10% of the radial line-force (Cranmer & Owocki 1995); but the equatorward flow speeds are similarly small, i.e. less than 100 km/s in the WCD model, or only a few percent of the maximum radial speed. Thus, while the radial line-force must be strong enough to overcome the stellar gravity to drive an outflow to terminal speeds of more than 1000 km/s, the poleward latitudinal line-force is unopposed by any other body force, and need only overcome inertial terms characterized by a modest, < 100 km/s equatorward drift. From this perspective, it thus seems clear that the derived nonradial forces should indeed be dynamically quite significant in redirecting the equatorward drift needed for a WCD.

Finally, although the 2D models here have an assumed azimuthal symmetry, there is nonetheless also a nonzero *azimuthal* component of the line-force, which again results from asymmetries in the line-of-sight velocity gradient. Because wind rotation speed declines with increasing radius, the velocity gradient toward the receding stellar hemisphere is greater than that toward the approaching hemisphere. Through eq. (7), this now implies a net line-force *against* the sense of rotation (Grinin 1978; Gayley & Owocki 2000). Its peak magnitude is roughly comparable to that for the poleward line-force, but this is sufficient to cause a modest wind spindown, characterized by about a 20% decrease in the specific angular momentum of the equatorial wind outflow beyond a few tenths of a stellar radius from the surface.

3.3. Equatorial Gravity Darkening and Bi-Stability

The above models all assume an uniformly bright surface, but for a rotating, radiative stellar envelope, the surface flux at each co-latitude θ is expected to scale with the centrifugally reduced effective gravity $F(\theta) \sim g_{eff}(\theta)$, leading to an "equatorial gravity darkening" (von Zeipel 1924). Figure 5c shows results for models that now include both nonradial forces and this gravity-darkened surface intensity. In this case, not only is there no disk, but the overall density in the equatorial regions is actually *reduced* relative to that at higher latitudes. This picture is in marked contrast with previous analyses that envisoned an enhanced equatorial mass loss [e.g., FA, PPK, and eqn. (6)]. Despite the reduced gravity near the equator, the wind mass flux there is now lower, owing to the reduced radiative flux associated with gravity darkening. The superposed vectors further show that the latitudinal velocity is again away from the equator, though with a somewhat lower magnitude than in figure 5b, owing to the reduced poleward force associated with the reduced radiative flux from the equator.

Results similar to those shown figure 5 have been obtained by Petrenz & Puls (2000) using a completely independent hydrodynamics code, incorporating also a more self-consistent treatment of the NLTE transfer to derive the latitudinal variation of the CAK parameters (α, k, and δ). Following on the discovery by Pauldrach & Puls (1990) of a "bi-stability" transition to stronger line driving in early B-stars with effective temperatures near 20,000 K, Lamers & Pauldrach (1991) proposed that in rapidly rotating B supergiants stars, a similar bi-stability jump associated with the equatorward decrease in effective temperature could now lead to an enhanced equatorial wind, suggesting this as a possible mechanism for the disks inferred from supergiant B[e] stars. A follow up analysis by Pelupessy et al. (2000) derived density enhancements up to a factor ten in 1D models, and argued that the addition of 2D WCD effects could provide the further factor of ten or more needed to approach the equatorial densities inferred empirically in B[e] supergiants. However, such a scenario seems to run counter to the simulations showing effective inhibition of equatorial wind compression by poleward forces. Thus far there have been no 2D dynamical models exhibiting such a bi-stabilty induced equatorial disk.

3.4. Rotational Shaping of Bipolar Outflows and Nebulae

These models showing that gravity darkening could result in enhancements in the polar mass loss from a rotating star led Owocki & Gayley (1997) to propose that such rotation effects could provide a natural explanation for the bipolar form of the outflows and nebulae in LBV stars like eta Carinae. In recent years this general idea has been followed up in further analyses and models by Maeder & Meynet (2000), Maeder & Desjacques (2001), and Dwarkadas & Owocki (2002). For the simple scaling of models that include gravity darkening, both the higher polar mass flux and higher polar flow speed fit the inferred conditions for eta Carinae's present day wind (Smith et al. 2003), as well as for the Homunculus nebuala (Smith 2002). Note however the giant eruption that lead to the Homunculus is estimated to have had a mass loss rate as high as 0.1-1 $M_\odot$/yr (Smith 2002). Because of the inherent saturaturation of lines at high density, this is well above (by a factor thousand or more) what could be driven by line opacity (Aerts et al. 2004). This thus raises serious doubts about

the relevance of the above results for rotating line-driven winds for explaining the bipolar form of such a dense nebular outflow.

However, recent work (Owocki et al. 2004) suggests that models of continuum driving moderated by the "porosity" of a spatially structured medium can retain the basic scalings that lead to a bipolar form, while also explaining both the high flow speed and extreme mass loss of the Homunculus. Just as for line-driven winds, the mass flux in this continuum-driven porosity model scales with the stellar radiative flux times a correction factor that is a function of the Eddington parameter, i.e., $\dot{m} \sim Ff[\Gamma]$. But for the standard von Zeipel (1924) gravity darkening law that $F(\theta) \propto g_{eff}(\theta)$, the local effective Eddington parameter along the stellar surface is *latitudinally constant*, implying then that the surface mass flux should again be directly proportional to the radiative flux. Since both the effective gravity and radiative flux are maximum at the rotational pole, this again shows that the mass flux should be strongest near the poles.

Similar arguments can be made for the latitudinal variation of the flow expansion speed. Again, the detailed results may depend on latitudinal components of the mass flow, radiation flux, and radiative force, and should eventually be analyzed through 2D models. But within the context of simple 1D scaling relations for both line-driven and porosity models, the outflow speed should follow the same approximate scaling with effective escape speed, which is proportion to the square root of the effective gravity. Since the effective gravity is highest toward the poles, we can expect the nebula expansion to be faster near the symmetry axis. Observations do indeed suggest that $v(\theta)$ for the polar lobes of the Homunculus nebula is roughly proportional to the simple latitudinal variation of escape speed from a rotating star (Smith 2002).

Overall, the expected faster polar flow speed can explain the generally prolate form of the expanding nebula, while the higher polar mass flux can explain the observationally inferred mass concentration near the polar symmetry axis. Thus, an attractive feature of the porosity-moderated continuum-driven formalism is that it preserves these key 1D flow scalings from line-driven models, while allowing extension to much larger mass loss rates. However, as noted, more complete 2D models should be developed to examine how these general scalings might be affected by latitudinal mass and radiation transport.

3.5. Fundamental Limitations on Radiative Driving of Optically Thick Disks

Finally, even apart from the specific effects that tend to inhibit equatorial disks in line-driven winds, there are also some quite fundamental reasons why radiative driving in general seems ill-suited to producing a geometrically thin, dense equatorial disk-like outflow. An essential point is that all the above analyses ignore multiple scattering effects. In optically thin winds this is well-justified, and even in dense, optically thick, but nearly spherical winds (such as occur in Wolf-Rayet stars), the trapping of radiation within the spherical envelope makes it possible for multiple scattering to maintain a strong outward radiative force. By contrast, as illustrated in figure 7, stellar radiation impingent on a geometrically thin, but optically thick disk should be scattered out of the disk plane after only one or two interactions, thus limiting the radiative acceleration to just the single scattering value. For a disk of transverse optical thickness

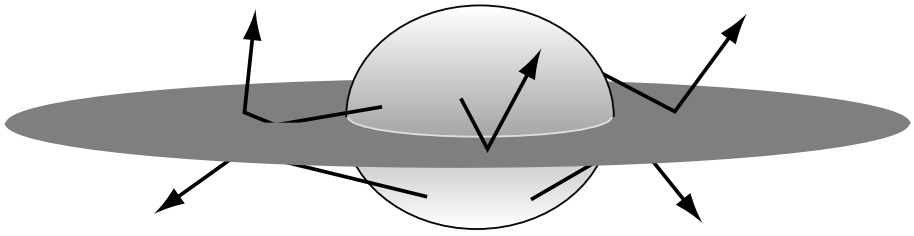

Figure 7. Schematic illustrating that stellar radiation (arrows) impingent on a geometrically thin but optically thick disk will tend to be reflected out of the disk plane after only one or two scatterings. This limits the radiative force to a single scattering value that is unlikely to overcome or even balance gravity. The upshot is that, regardless of the opacity available, radiation seems inherently ill-suited to supporting or driving a dense equatorial disk or disk outflow.

$\tau > 1$, the net result is to reduce the radiative acceleration by about a factor $1/\tau$ compared to the optically thin acceleration $\kappa F/c$. If the opacity κ has an associated Eddington parameter $\Gamma \equiv \kappa F/gc$, then unless $\Gamma \gg 1$, the radiative acceleration of the disk will not be able overcome, or indeed even statically balance, the inward gravitational acceleration g. The upshot is that, regardless of the opacity available, it seems radiation is inherently ill-suited to driving or even supporting a dense equatorial disk or disk outflow.

So instead of radiative driving, it seems a more likely explanation for the dense equatorial disks inferred in Be and B[e] stars might be direct *centrifugal ejection* from a near-critically rotating surface. When gravity darkening effects are taken into account, it seems that the photospheric line broadening observed in Be stars may be consistent with near-critical rotation [Townsend et al. (2004), but see also Cranmer (2005)]. If the equatorial rotation speed is within about a sound speed of the critical value, then even minor disturbances in the stellar photosphere, e.g. pulsations, could propel material in a near-star Keplerian orbit, whereupon it could diffuse outward as part of a "viscous decretion disk" (Lee et al. 1991). Such a decretion disk paradigm has been applied quite successfully to Be stars, and may also be relevant for B[e] supergiants. Moreover, the dense equatorial outflows observed in both Be and B[e] stars might arise from surface ablation of a Keplerian disk by the stellar radiation. Indeed, radiative destruction of the relatively weak disks in Be stars may account for the episodic disappearance of Be disk emission on time scales of a year or so. Perhaps also the "equatorial skirt" of eta Carinae represents the remnants of an centrifugally ejected disk that was disrupted by the bright radiation and dense outflow of the 1840-50 giant eruption.

Overall then, quite apart from the initial expectations that rotation would enhance the equatorial components of radiatively driven mass loss, we see that the tendency is instead to drive an enhanced bipolar mass loss, with radiation perhaps even playing a key role in disk destruction rather than creation.

Acknowledgments. This work was done with partial support of NSF grants AST-0097983 and AST-0507581. I thank Tom Madura and Allard-Jan van Marle for helpful comments on the manuscript.

References

Aerts, C., & Lamers, H. J. G. L. M. 2003, A&A, 403, 625
Aerts, C., Lamers, H. J. G. L. M., & Molenberghs, G. 2004, A&A, 418, 639
Bjorkman, J. E., & Cassinelli, J. P. 1993, ApJ, 409, 429
Bjorkman,J. E. 1999, Variable and Nonspherical Stellar Winds in Luminous Hot Stars, B. Wolf, O. Stahl, and A. Fullerton, eds., IAUC 169, Lecture Notes in Physics 523, Springer, p. 121
Castor, J. I., Abbott, D. C., & Klein, R. I. 1975, ApJ, 195, 157 (CAK).
Cranmer, S. R., & Owocki, S. P. 1995, ApJ, 440, 308
Cranmer, S. R. 2005, ApJ, 634, 585
Curé, M. 2004, ApJ, 614, 929
Curé, M., & Rial, D. F. 2004, A&A, 428, 545
Curé, M., Rial, D. F., & Cidale, L. 2005, A&A, 437, 929
Dwarkadas, V. and Owocki S. 2002, ApJ, 581, 1337.
Friend, D. B., & Abbott, D. C. 1986, ApJ, 311, 701 (FA)
Gayley, K. G. 1995, ApJ, 454, 410
Gayley, K. G., & Owocki, S. P. 2000, ApJ, 537, 461
Grinin, A. 1978, Sov. Astr., 14, 113
Hanushik, R. W. 1995, A&A, 295, 423.
Ignace, R., Cassinelli, J. P., and Bjorkman, J. E. 1996, ApJ, 459, 671
Lamers, H. J. G., & Pauldrach, A. W. A. 1991, A&A, 244, L5
Lee, U., Osaki, Y., & Saio, H. 1991, MNRAS, 250, 432
Madura, T., Owocki, S., & Feldmeier, A. 2006, ApJ, submitted
Maeder, A., & Meynet, G. 2000, A&A, 361, 159
Maeder, A., & Desjacques, V. 2001, A&A, 372, L9
Owocki, S. and Gayley, K. 1997, *Luminous Blue Variables: Massive Stars in Transition*, A. Nota and H. Lamers, eds., A.S.P. Conf. Ser. 120, 121.
Owocki, S. 2006, Stars with the B[e] Phenomenon, ASP Conference Series, M. Kraus and A. Miroshnichenko, eds., in press.
Owocki, S. P., Cranmer, S. R., & Blondin, J. M. 1994, ApJ, 424, 887
Owocki, S. P., Cranmer, S. R., & Gayley, K. G. 1996, ApJ, 472, L115
Owocki, S. P., Gayley, K. G., & Shaviv, N. J. 2004, ApJ, 616, 525
Pauldrach, A., Puls, J., & Kudritzki, R. P. 1986, A&A, 164, 86 (PPK)
Pauldrach, A., & Puls, J. 1990, A&A, 237, 409.
Pelupessy, I., Lamers, H. J. G. L. M., & Vink, J. S. 2000, A&A, 359, 695
Pereyra, N. A., Owocki, S. P., Hillier, D. J., & Turnshek, D. A. 2004, ApJ, 608, 454
Petrenz, P., & Puls, J. 2000, A&A, 358, 956
Poe, C. H. 1987, Ph.D. thesis, Univ. of Wisconsin
Poe, C. H., & Friend, D. B. 1986, ApJ, 311, 317
Rivinius, T., Stefl, S., and Baade, D. 1999, A&A, 348, 831.
Savonije, G.J. 1998, in *Cyclical Variability in Stellar Winds*, L. Kapers and A. Fullerton, eds., Springer: Berlin, p. 337
Savonije,G.J., and Heemskerk,M.H.M. 1993, A&A, 276, 409
Smith, N. 2002, MNRAS, 337, 1252
Smith, N., Davidson, K., Gull, T. R., Ishibashi, K., Hillier, D. J. 2003, ApJ, 586, 432
Telting,J., Heemskerk,M., Henrichs,H., and Savonije,G. 1994, A&A, 288, 558
Townsend, R. H. D., Owocki, S. P., & Howarth, I. D. 2004, MNRAS, 350, 189
von Zeipel, H. 1924, MNRAS, 84, 665